Available online at www.sciencedirect.com
ScienceDirect
Applied Surface Science 253 (2006) 639–645
applied surface science
www.elsevier.com/locate/apsusc

Surface morphology of Dy_xO_y films grown on Si

K. Lawniczak-Jablonska [a,*], N.V. Babushkina [b], E. Dynowska [a], S.A. Malyshev [b], L.I. Romanova [b], D.V. Zhygulin [b], T. Laiho [c]

[a] Institute of Physics, Polish Academy of Sciences, Al. Lotnikow 32/46, 02 668 Warsaw, Poland
[b] Institute of Electronics, National Academy of Sciences of Belarus, Logoiski trakt 22, 220090 Minsk, Belarus
[c] Laboratory of Materials Science, Department of Physics, University of Turku, FIN-20014 Turku, Finland

Received 14 June 2005; received in revised form 16 December 2005; accepted 22 December 2005
Available online 30 January 2006

Abstract

The crystalline structure and surface morphology of Dy_xO_y dielectric films grown on Si substrates were studied by grazing incidence diffraction and absorption with use of synchrotron radiation and by atomic force microscopy. The crystalline structure and the roughness of Dy_xO_y films were found to be strongly dependent on the deposition rate. The dielectric-silicon interface depends on the type of gas used in the annealing process. Moreover, results from the near edge X-ray absorption studies, have revealed that none of the examined films has a stoichiometry close to the Dy_2O_3. The level of stoichiometry is determined by the technological conditions. Nevertheless, MOS structures with Dy_xO_y films (EOT $\sim$ 23 Å) have shown a rather good Dy_xO_y-Si interface properties, which can be further improve by thermal annealing, and introducing of several additives, therefore Dy_xO_y films can be considered as suitable candidates for gate dielectric in MOS devices.
© 2006 Elsevier B.V. All rights reserved.

PACS: 85.50; 61.10.H; 78.70.D

Keywords: Dielectrics; Dysprosium oxide; X-ray diffraction; X-ray absorption; Atomic force microscopy

1. Introduction

The continual miniaturization of the metal-oxide-semiconductor (MOS) devices requires the replacement of SiO_2 with dielectrics with high-k constant. In the last decade much attention has been devoted to the study of high-k dielectrics (Al_2O_3 [1], HfO_2 [2–4], ZrO_2 [5], Y_2O_3 [6,7], La_2O_3 [1,6]) suitable for producing microelectronic devices and integrated circuits and featuring properties equivalent to very thin SiO_2.

The dielectric films with high-k must satisfy many requirements. A very important requirement is that the atomic structure of the film should be amorphous and has to have low roughness of the dielectric-silicon interface.

It is well known that the formation of crystalline grains in the dielectric films leads to oxygen diffusion along grain boundaries during thermal processing. This can result in the growth of interfacial SiO_x layer and increase the possible equivalent SiO_2 thickness that should have the high-k materials. Moreover, the grain-boundary diffusion of other impurities deteriorates the electrical performance of the MOS devices. A high leakage current is observed in the polycrystalline dielectric films due to additional leakage path along the grain boundaries [2,3]. Nevertheless, it is worth noting that polycrystallinity in the oxide films of lanthanides La_2O_3 and Y_2O_3 does not result in unacceptably high leakage currents [6,7].

Regarding the roughness it was found that MOS devices with the ultra-thin gate dielectrics are very sensitive to the roughness of the dielectric film surface and dielectric-silicon interface. The increase of the dielectric-silicon interface roughness results in an increased charge state density at the interface D_{it}, and therefore, in the scattering of the carriers on the silicon surface. The scattering becomes dominant in carrier transport of MOS field-effect transistor (FET) and degrades MOS FET channel mobility [8–10]. Moreover, the roughness degrades the time-dependent dielectric breakdown characteristics of MOS capacitors, and increases the tunneling current through the dielectric [11]. Therefore, there is a need for elaborating of technology of growing the smooth, amorphous or single crystal very thin layers of dielectric oxides.

* Corresponding author. Tel.: +48 22 8436034; fax: +48 22 8436034.
E-mail address: jablo@ifpan.edu.pl (K. Lawniczak-Jablonska).

0169-4332/$ – see front matter © 2006 Elsevier B.V. All rights reserved.
doi:10.1016/j.apsusc.2005.12.150

Among the high-k dielectrics under consideration, Dy_xO_y is promising due to its relatively high dielectric constant ($k = 12$) as compared to SiO_2 ($k = 3.9$). There is not much reported about possibility to use this dielectric for producing the thin layer. Therefore, we have studied the crystalline structure and the surface morphology of the thin Dy_xO_y films, produced on Si by relatively simple technology. To examine the crystalline structure and range of ordering in Dy_xO_y layers, prepared at different conditions, the synchrotron radiation diffraction and absorption were used. To study the roughness and morphology of the surface and interface AFM was employed. Next, to check the electrical properties of the layer the MOS structure was constructed from the film grown at the same conditions as sample 1, with the best properties of the surface, and the high-frequency capacitance–voltage (C–V) characteristics were measured.

2. Experimental

The p-type and n-type Si wafers with (1 0 0) orientation were used as substrates. They were cleaned by organic solvent, etched in a solution of NH_4OH:H_2O_2:H_2O (1:1:7) and then rinsed in running deionized water. The Dy_xO_y films for different samples were obtained by Dy evaporation in a mixed Ar–6% O_2 atmosphere. The deposition was performed onto non-heated Si substrates. The preliminary pressure in the vacuum chamber was $\sim 2 \times 10^{-6}$ Torr. Then, the Ar mixed with O_2 was admitted into the preparation chamber through a leak valve. The final pressure in the chamber was 7×10^{-5} or 1×10^{-4} Torr depending on sample. Thermal annealing of all films was conducted at the temperature $T_{ox} = 500\ ^\circ C$ during 7 min in a dry oxygen stream (samples 1, 2, and 4) or 8 min in argon stream (sample 5). The deposition rate was $\sim$1 Å/s for the samples 1 and 6, respectively, and 2.4–3 Å/s for other samples. The Dy_xO_y films under investigation had thickness ranging from 50 to 120 Å as was found by depth profile Auger spectroscopy. Scanning Auger Microprobe (SAM) PHI 610 Perkin-Elmer was used for measuring Auger depth profile of elements distribution with 2 keV Ar^+ ions and 0.5 min sequence of sputtering. The conditions of sample preparation are summarized in Table 1. The conditions of samples preparation were changed in the way, which allows to check the influence of several factors. In samples 1 and 2 the evaporated time and current were changed and it appears that current has important influence on the film thickness and decreasing of time did not compensate the increase of current. The influence of gas environment was studied in samples 4 (O_2) and 5 (Ar). The influence of active gas pressure can be seen in comparison of properties of samples 1 and 6, and 2 and 4, respectively.

The crystalline structure of the Dy_xO_y films was examined using synchrotron radiation diffraction in the grazing incidence diffraction (GID) mode with a powder diffractometer installed at beamline B2 in HASYLAB, Hamburg. A parallel beam, monochromatized with Ge (1 1 1) double-crystal monochromator and a diffracted-beam collimator built of parallel foils, was used. In this method the monochromatic beam (here the wavelength $\lambda = 1.119949$ Å) strike the sample at very small, constant angle of incidence α (here $\alpha = 0.75^\circ$). The diffracted intensity was recorded by detector rotated around the sample in a large range of 2θ angles (where 2θ angle is the angle between incident and diffracted beams for given lattice planes family). This geometry of measurement allows to investigate very thin layer of the sample.

X-ray absorption near edge spectra (XANES) at Dy L-edges were measured at the room temperature in HASYLAB at beamline A1. All samples were electrically isolated from the spectrometer and drain current from the samples was measured (total yield mode).

The morphology of the Dy_xO_y films and Dy_xO_y-Si interfaces was studied using the Atomic Force Microscopy (AFM) Auto Probe CP, Park Scientific Instruments with the gold coated silicon nitride cantilevers to take contact-mode images.

The MOS capacitor with the Dy_xO_y film was fabricated on (1 0 0) oriented, 1 Ω cm, p-type Si substrate. The Dy_xO_y film was produced with low deposition rate and annealed for 7 min at $T_{ox} = 500\ ^\circ C$ in dry oxygen stream (as sample 1). In gate, electrodes of area 1.6×10^{-3} cm^{-3} were vacuum evaporated through a metal mask. The high-frequency capacitance–voltage (C–V) characteristics were measured at 1 MHz. The sweep rate was 0.07–0.7 V/s.

3. Results and discussion

Due to the fact that Dy_xO_y layers being investigated were very thin (50–120 Å) it was not possible to obtain any meaningful diffraction pattern by conventional X-ray diffraction techniques. Only the use of GID geometry and synchrotron radiation resulted in registration of some diffraction peaks from the layers (Fig. 1). The quality of the diffraction patterns indicates that level of film crystallinity is variable and is a function of the technological conditions. On the base of

Table 1
The condition of samples preparation

No.	Pressure (Ar/O_2) (Torr)	Evaporator current (A)	Evaporation time (s)	Layer thickness (Å)	Deposition rate (Å/s)	Oxidation time (min)	Gases environment
1	7×10^{-5}	320	60	63	~1	7	O_2
2	7×10^{-5}	330	40	119	~3	7	O_2
4	1×10^{-4}	330	40	98	~2.4	7	O_2
5	1×10^{-4}	330	40	105	~2.6	8	Ar
6	1×10^{-4}	320	60	56	~0.9	7	O_2

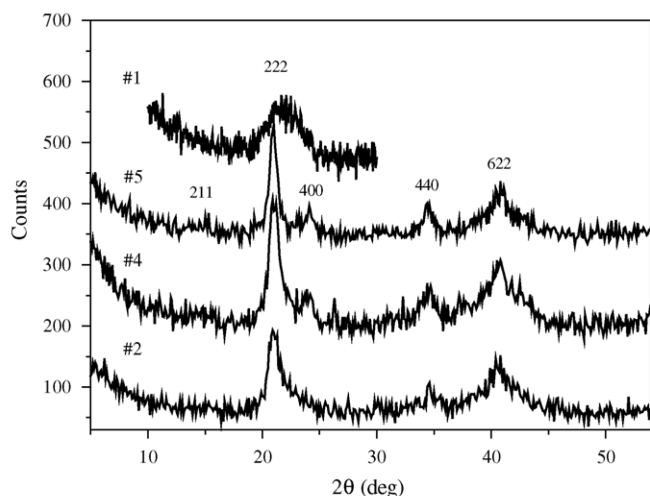

Fig. 1. Grazing incident diffraction patterns for different Dy_xO_y layers.

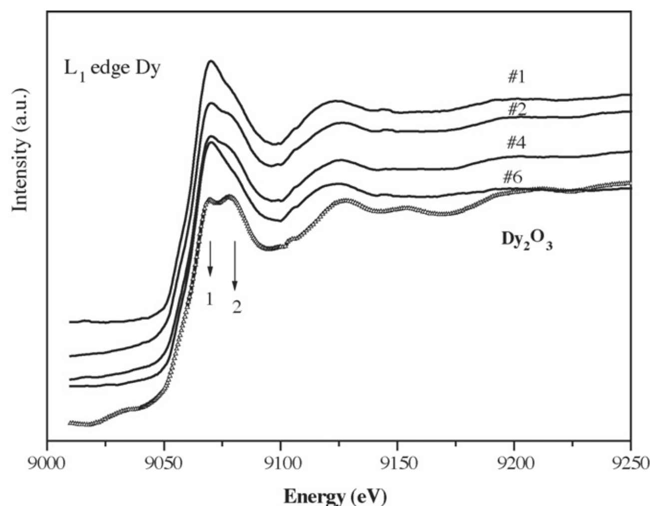

Fig. 2. L_1 edges of Dy in Dy_xO_y layers and Dy_2O_3 powder.

obtained diffraction patterns we could identify the crystal structure of the films as Dy_2O_3, cubic of $I\,a\,\bar{3}$ space group with lattice parameter $a = 10.665$ Å, (according to the JCPDS-ICDD, 22-0612). The relative intensities and shapes of diffraction lines differ somewhat from ICDD powder diffraction data, which is attributed to not fully statistical distribution of crystallites inside the investigated layers. Moreover, the GID method does not give information on preferred orientation of the crystallites as well as on their sizes—therefore such effects are not discussed. The aim of presented diffraction studies was qualitative estimation of a crystal state of studied layers.

On the base of GID studies one can say that the Dy_xO_y films obtained with high deposition rate have the best crystalline structure (samples 2, 4, and 5). The thickness of these films is around 100 Å (Table 1). The decreasing of the deposition rate leads to deterioration of the Dy_2O_3 film crystalline structure (Fig. 1, sample 1). A pronounced decrease in the intensity, broadening and shift of the 2 2 2 peak is observed for the sample 1. There are no other peaks in the diffraction pattern of this sample, which indicates that the crystallites size is extremely small. For sample 6 grown under conditions similar to those for sample 1 but at different active gas pressure, no diffraction peaks were detected, which implied that the film is an amorphous. Moreover, the quality of crystalline structure does not depend much on the gases used in the annealing process (samples 4 and 5). The interplanar spacings calculated from the 2θ positions of the peaks registered at the diffraction patterns and these values given in the JCPDS-ICDD, 22-0612 data are presented in Table 2. The fact that the peaks are broad indicates that the crystal quality of the films is not good. Nevertheless, the crystalline structure formed is characteristic for Dy_2O_3 phase.

The shape of XANES is a fingerprint of the compounds formed [12,13], and the appearance of the fine structure in a spectrum is evidence of formation of long-range ordering [14]. Therefore, the L edges of Dy were measured for films together with the stoichiometric Dy_2O_3 powder. This method is sampling all volume of layer. To get information about the range of ordering around the Dy atoms, spectra of L_1 edge (presented in Fig. 2), and spectra for L_3 edge (Fig. 3) were examined. Changes observed in the shape of L_1 edges (Fig. 2), indicate that the oxides formed have different levels of stoichiometry but none of them is Dy_2O_3. The fine structure seen in L_1 edges of Dy_2O_3 was not found in samples 1 and 6 indicating the absence of long-range order in these samples, in agreement with results of diffraction studies. The reversed

Table 2
The results of phase identification

Diffraction peak *h k l*	Interplanar spacing *d* (Å) (experimental values)	Interplanar spacing *d* (Å) (JCPDS-ICDD, 22-0612)	Intensity (JCPDS-ICDD, 22-0612)
2 1 1	4.34	4.350	16
2 2 2	3.080	3.079	100
4 0 0	2.684	2.666	40
4 4 0	1.885	1.885	45
6 2 2	1.611	1.608	35

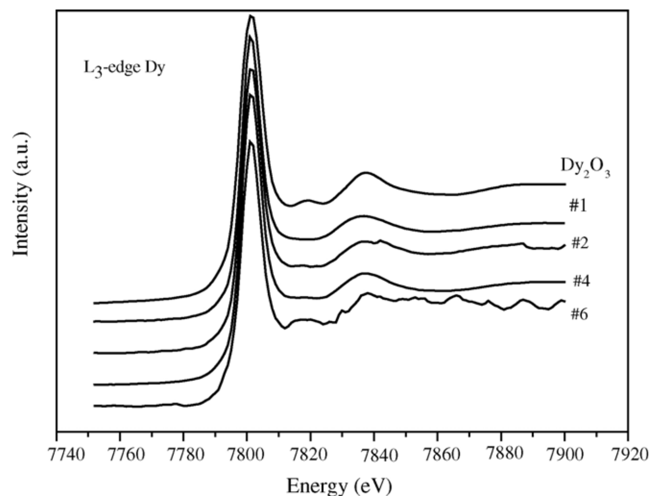

Fig. 3. L_3 edges of Dy in Dy_xO_y layers and Dy_2O_3 powder.

intensity in the two peak structures at the first maximum marked 1 and 2 (Fig. 2) for other samples, is an evidence of different stoichiometry than that of Dy_2O_3. In L_1 edge the p-symmetry states in the conduction bond are examined, and it can be seen that these states are very sensitive to the level of ordering in the sample. The d-symmetry states investigated in L_3 edge are almost the same for all different films (Fig. 3). Therefore, the d-states are not so much sensitive to the ordering in the sample because they are much more localized than the p-symmetry states. There is difficulty to get more quantitative information from the XANES examination. Examination of the extended X-ray absorption structure (EXAFS) can provide more quantitative information about the level of stoichiometry but, unfortunately, the diffraction peaks from the thin layer induced additional structure to the EXAFS, and strongly influenced the results of the analysis. The other spectroscopic method suitable for quantitatively examination of the stoichiometry is X-ray photoelectron spectroscopy, but this technique is surface sensitive. Layers were exposed to the air and surface was strongly contaminated with carbon and adventitious oxygen. The Ar ion sputtering changed the content of elements due to different sputtering rate of Dy and O atoms. Moreover, the 1s line of oxygen had two component structure indicating on different chemical bounding of analyzed oxygen. No significant differences between ratios of Dy to oxygen at the surface in investigated samples were detected.

The AFM results of the studies of Dy_xO_y films morphology are presented in Figs. 4–7. The three dimensional images of the Dy_xO_y films on samples 1 and 5 are shown in Fig. 4a–c. The morphology of oxide films varies significantly. The surface of the sample 1 is smooth even at the high magnification (Fig. 4b). The height profile was made (Fig. 5) from four different lines at the surface of this sample for a quantitative estimation of the roughness of formed surface. The mean height of the roughness was found to be close to 15 Å. The example of height profiles for samples 4 and 5 are shown in Fig. 6. Analysis of these profiles shows that the Dy_xO_y grows in the form of crystallites with the height of about 100 ± 20 Å and the width at the bottom of 0.3 ± 0.1 μm. Therefore, the morphology of Dy_xO_y films strongly depends on the deposition rate. In the case of low deposition rate (sample 1) a fine-grained structure close to amorphous one was obtained, and in the case of high deposition rate (samples 5 and 4) polycrystalline structure with large grain sizes was grown. These results are in agreement with the XRD data.

The AFM images taken from samples 1 and 6 and samples 2 and 4 were very similar, therefore, the pressure change of active gas in the vacuum chamber from 1×10^{-4} to 7×10^{-5} Torr during the film deposition, has no considerable effect on the Dy_xO_y films morphology.

To judge the effect of post-deposition annealing environment on the Dy_xO_y surface morphology one should compare samples 4 and 5 (Fig. 6). Both samples have thickness of about 100 Å and were deposited at the same high rate and high gas pressure, but sample 4 was annealed in O_2 and sample 5 in Ar. In the case of oxygen annealing, crystallites are distributed uniformly and have about similar height. The difference

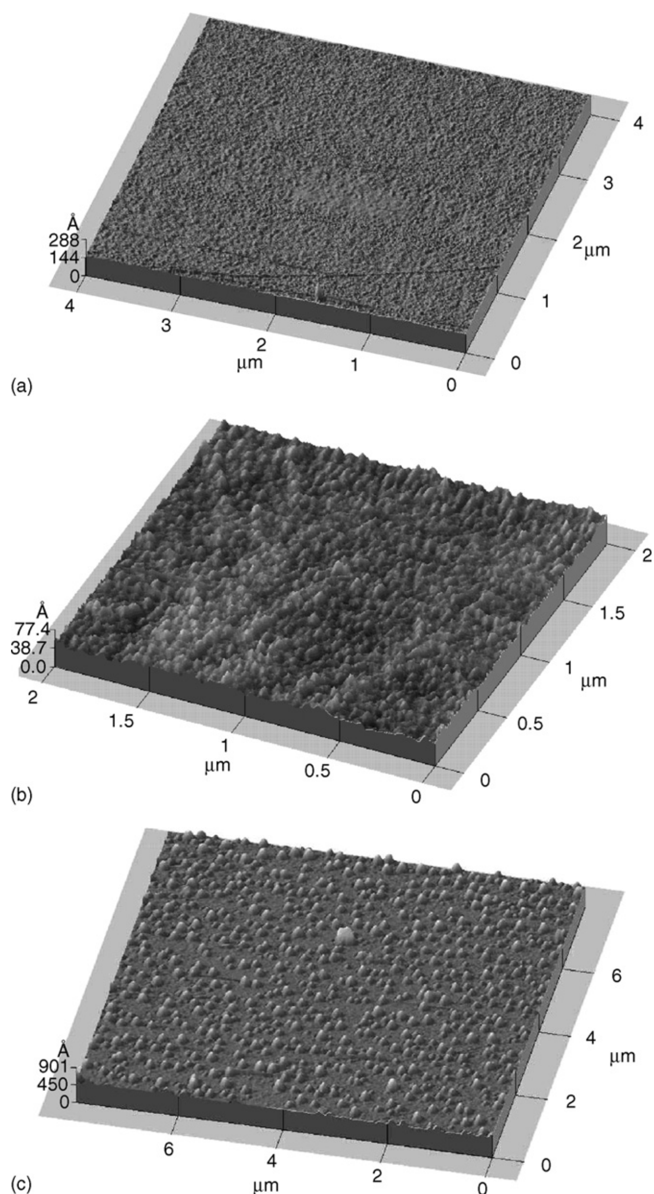

Fig. 4. AFM three-dimensional images of Dy_xO_y film surfaces: (a) sample 1 from 4 μm × 4 μm surface, (b) sample 1 from 2 μm × 2 μm surface, and (c) sample 5 from 8 μm × 8 μm surface.

between grains height (Fig. 6a) is about 40 Å. In the case of Ar annealing the non-homogeneity of height distribution is larger.

To investigate the morphology of the interface between the Dy_xO_y films and silicon surface, the oxide films were completely removed by ion beam etching (2 keV Ar^+), and the exposed Si surfaces were studied by AFM. One cannot exclude that etching by ion can, to some extend, influence the surface morphology, because of different sputtering rate of elements, but it can be assume that this influence is the same in all investigated samples, and for our studies the differences between samples are most important. Moreover, examination of Dy Auger line during sputtering procedure gives evidence that Dy film was completely removed. The AFM images and height profiles for interface of samples 1, 4 and 5 are shown in Fig. 7. It is seen that for sample 1 peaks and valleys of ± 8 Å height

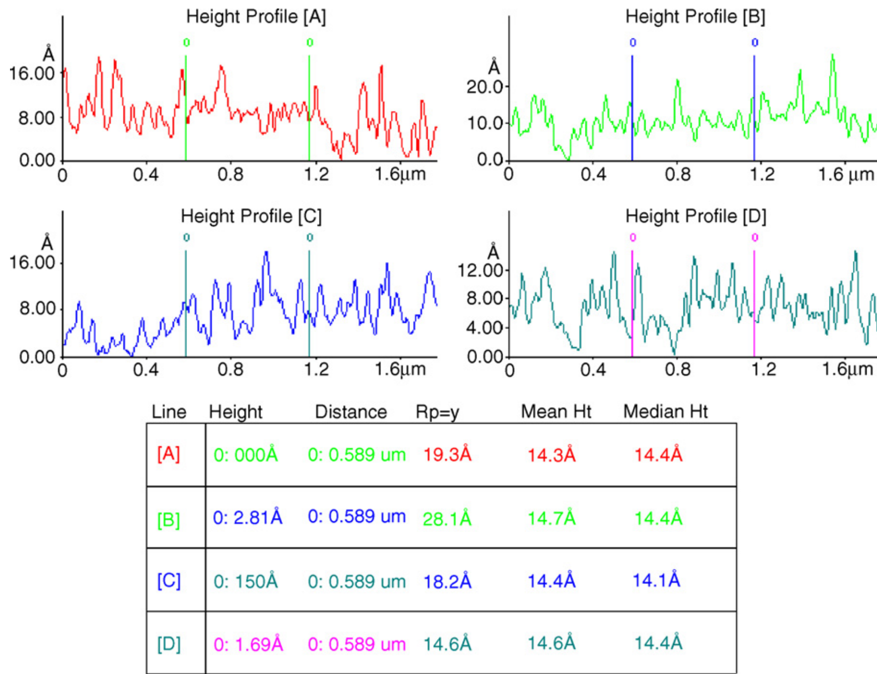

Line	Height	Distance	Rp=y	Mean Ht	Median Ht
[A]	0: 000Å	0: 0.589 um	19.3Å	14.3Å	14.4Å
[B]	0: 2.81Å	0: 0.589 um	28.1Å	14.7Å	14.4Å
[C]	0: 150Å	0: 0.589 um	18.2Å	14.4Å	14.1Å
[D]	0: 1.69Å	0: 0.589 um	14.6Å	14.6Å	14.4Å

Fig. 5. The roughness of the surface of sample 1 taken from the profile measurements along four lines.

remained after sputtering. For sample 4, a smooth surface with individual randomly distributed peaks of about 60 Å height was found, and in case of sample 5 increasing roughness of the interface was observed.

The results of investigation of the electrical properties of samples are shown in Fig. 8. The high-frequency *C–V* curves of the In-Dy_xO_y-pSi capacitor were measured and simulated. The indicated equivalent oxide thickness (EOT) of 23 Å was extracted using Berkeley simulated program, taking into account the quantum mechanical correction [15]. EOT is defined as the thickness extracted from accumulation capacitance of the *C–V* curve assuming that the permittivity *k* of the film is that of SiO_2 ($k = 3.9$). The good agreement between measured and simulated *C–V* curves indicated the low interfacial traps at the Dy_xO_y-Si interface. There is a small injection-type hysteresis ($\Delta V < 8$ mV) in the *C–V* curve connected with the charge carrier trapping at the interface. The low density of interface traps at the Dy_xO_y-Si interface and small injection-type histeresis in the *C–V* curve confirm that amorphus sample 1 has the smooth Dy_xO_y-Si interface. The leakage current is found to be about $\sim 3 \times 10^{-3}$ A/cm^2 at the $V_g - V_{fb} = -1$ V. The leakage current of SiO_2 film with the same equivalent thickness is about 8×10^{-4} A/cm^2 at the 1 V + $|V_{fb}|$ at accumulation [16]. Further improvement of the Dy_xO_y film leakage current may be expected by means of thermal annealing.

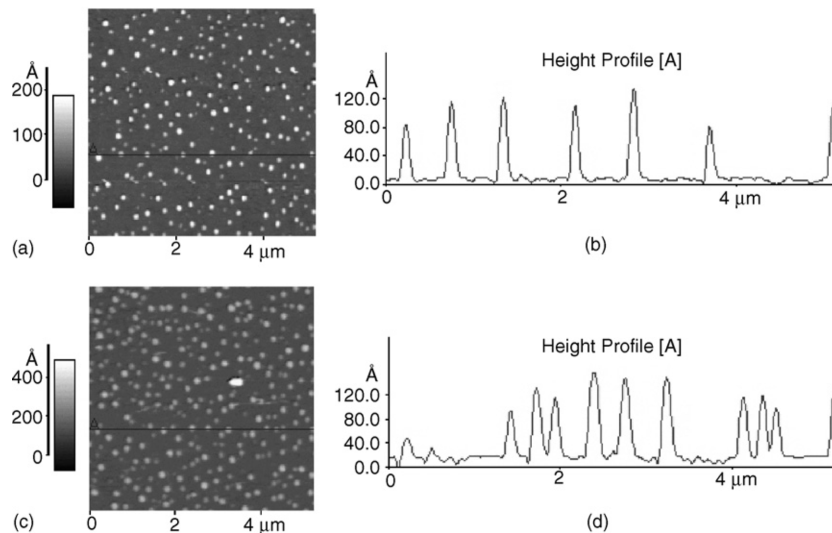

Fig. 6. AFM images and height profiles of the Dy_xO_y films surfaces: (a and b) sample 4; (c and d) sample 5.

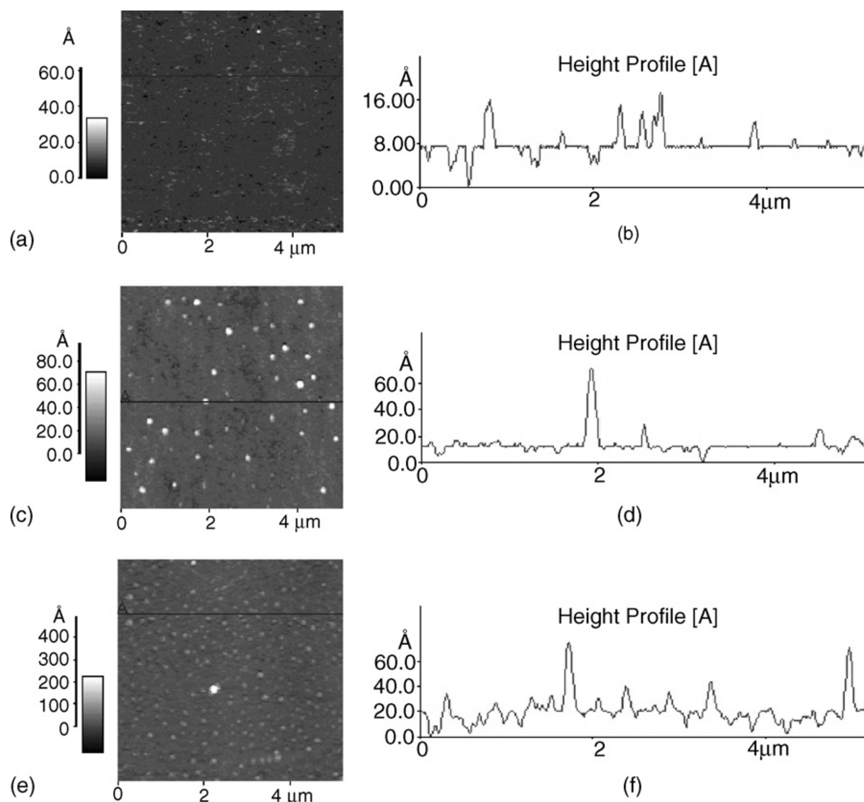

Fig. 7. AFM images and height profiles of silicon surfaces after the complete ion-beam stripping of the Dy_xO_y films: (a and b) sample 1, (c and d) sample 4, and (e and f) sample 5.

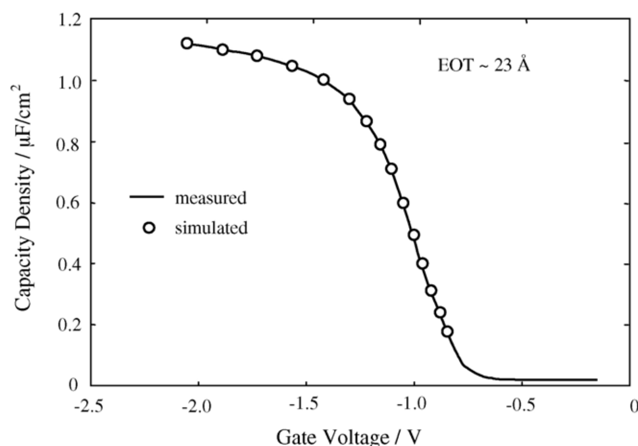

Fig. 8. The high frequency measured and simulated capacitance density vs. gate voltage of the In-Dy_xO_y-pSi capacitor constructed from the film produced at the same technological condition as sample 1.

4. Conclusion

The possibility to produce the thin amorphous films of Dy_xO_y with the roughness level of about 15 Å and with a smooth dielectric-silicon interface (roughness 8 Å) was demonstrated. The film morphology strongly depends on the deposition rate. Low deposition rates results in the growth of almost amorphous film, while an increase of the deposition rate leads to formation of crystallites inside the film with the base size of about 0.3 µm and the height of about 100 Å. The crystallographic structure of the crystallites was determined as the phase Dy_2O_3, cubic of $Ia\bar{3}$ space group with lattice parameter $a = 10.665$ Å, even though the stoichiometry of all films differs from that of Dy_2O_3. The annealing in the argon leads to the increase of the interface dielectric-silicon roughness.

The MOS structures with Dy_xO_y films (EOT ~ 23 Å) have shown a rather good Dy_xO_y-Si interface properties therefore, Dy_xO_y films prepared by thermal evaporation in mixed Ar-O_2 atmosphere at low deposition rate, followed by annealing in oxygen, can be considered as suitable candidates for gate dielectric in MOS devices. Obviously, more technological work is needed to improve the electrical properties of Dy_xO_y films.

Acknowledgements

This work was partially supported by the State Committee for Scientific Research (Republic of Poland) (*Grant No. 72/E-67/SPB/5.PR UE/DZ 27/2003-2005*) and by G1MA-CI-2002-4017 (CEPHEUS) and the IHP-Contract HPRI-CT-2001-00140 of the European Commission.

References

[1] A. Chin, Y.H. Wu, S.B. Chen, C.C. Liao, W.J. Chen, Symp. Very Large Scale Integration Technol. Symp. Digest (2000) 16.

[2] G.D. Wilk, R.M. Wallace, Appl. Phys. Lett. 74 (2000) 2854.
[3] W.J. Zhu, T. Tamagawa, M. Gibson, T. Furukawa, T.P. Ma, IEEE Electron Device Lett. 23 (2002) 649.
[4] C.H. Lee, J.J. Lee, W.P. Bai, J.H. Sim, X. Lei, R.D. Clark, Y. Harada, M. Niwa, D.L. Kwong, Symp. Very Large Scale Integration Technol. Symp. Digest (2002) 82.
[5] R. Nieh, R. Choi, S. Gopalan, K. Onishi, C.S. Kang, H.-J. Cho, S. Krishnan, J.C. Lee, Appl. Phys. Lett. 81 (2002) 1663.
[6] S. Guha, E. Cartier, M.A. Gribelyuk, N.A. Bojarczuk, M.C. Copel, Appl. Phys. Lett. 77 (2000) 2710.
[7] L.-A. Ragnarsson, S. Guha, M. Copel, E. Cartier, N.A. Bojarczuk, J. Karasinski, Appl. Phys. Lett. 78 (2001) 4169.
[8] C.-H. Lin, F. Yuan, C.-R. Shie, K.-F. Chen, B.-C. Hsu, M.H. Lee, W.W. Pai, C.W. Liu, IEEE Electron Device Lett. 23 (2002) 431.
[9] T. Yamanaka, S.J. Fang, H.-C. Lin, J.P. Snyder, C.R. Helms, IEEE Electron Device Lett. 17 (1996) 178.
[10] J. Koga, S. Takagi, A. Toriumi, Int. Electron Devices Meet. Digest (1994) 475.
[11] T. Nakanishi, S. Kishii, A. Ohsawa, Very Large Scale Integration Technol. Sympos. Digest (1989) 79.
[12] D.C. Koningsberger, R. Prins, X-Ray Absorption Spectroscopy, Chemical Analysis, vol. 92, Wiley, New York, 1988.
[13] K. Lawniczak-Jablonska, T. Suski, I. Gorczyca, N.E. Christensen, J. Libera, J. Kachniarz, P. Lagarde, R. Cortes, I. Grzegory, Appl. Phys. A 75 (2002) 577.
[14] P. Sainctavit, J. Petiau, M. Benfatto, C.R. Natoli, Phys. B 158 (1989) 347.
[15] QM CV Simulator, UC Berkeley Device Group. http://www-device.eecs.berkeley.edu/qmcv/index.html.
[16] M. Yang, E. Gusev, M. Ieong, O. Gluschenkov, D. Boyd, K. Chan, P. Kozlowski, C. D'Emic, R. Sicina, P. Jamison, A. Chou, IEEE Electron Device Lett. 24 (2003) 339.